Comparative Medicine
Copyright 2010
by the American Association for Laboratory Animal Science

Vol 60, No 5
October 2010
Pages 374–379

Morphometric Comparison of the Lumbar Cancellous Bone of Sheep, Deer, and Humans

Yang Wang,[1,3] Guomin Liu,[2] Ting Li,[1] Yanlong Xiao,[1] Qing Han,[1] Randong Xu,[1] and Youqiong Li[1,*]

To investigate the feasibility of using deer and sheep as animal models for the human spine, we compared the microarchitectural dimensions of the deer and sheep spines and with human data. To this end, we adopted the traditional bone tissue morphometric method, using figure analysis software for quantitative analysis of 2D images of bone tissue. Compared with those of humans, the lumbar cancellous bone of deer and sheep has higher microarchitectural indices, more densely packed bone trabeculae, lower porosity, and higher bone mass. Despite specific differences in various morphologic indices, the anisotropy of lumbar cancellous bone in deer and sheep shows the same trend as that in humans.

Implants comprising engineered bone tissue, internal fixation systems, and artificial joints have become important therapeutic tools in spinal surgery. After insertion, the primary factors that influence the therapeutic success of spinal implants are their biocompatibility and mechanical properties.[32] The insertion of spinal implants into vertebrae diminishes the integrity of the vertebral trabecular bone at the bone–implants interface, potentially leading to insufficient mechanical stability at the interface and subsequent loosening of the implant and loss of the correction due to fixation. Likely the more similar the surface microarchitecture of implants is to the cancellous bone into which they are implanted, the more biocompatible the implant. Spinal implants whose surface microarchitecture mimics that of cancellous bone may lead to improved stability as trabeculae grow into and adhere to the implant. Therefore analyzing the microarchitecture of vertebral cancellous bone is important not only in terms of theoretical research but also for the clinic practice of spinal surgery.

In addition, the advancement of spinal surgery depends on the progress of laboratory animal science. The animal models used most frequently in spine research include calves, goats, and sheep;[13,23,30,31] dogs have been involved infrequently.[2] However, the recent outbreaks of bovine spongiform encephalopathy, avian influenza, SARS, and influenza A (H1N1) and the possible hazards to personnel working with potentially contaminated tissues have made the selection of animal models for spine research more rigorous than ever.[29] Because of these concerns, some countries have imposed strict regulations on the use of sheep and calves for experimental work.[15]

We chose sheep (Chinese merino) and deer (*Cervus nippon* Temminck) for the research subjects for the current study of the microarchitecture of vertebral cancellous bone. The sheep (genus sheep, species Chinese Merino), progeny of a cross between an Australian Merino ram and Boer Wentz ewe, have the advantages of stable heredity and small interindividual differences. Because of the easy to obtain and less stringent governmental regulations regarding their use, Currently, Chinese merino are the most suitable sheep for experiments in our country.

Adult red deer may be an appropriate alternative model of the human spine. Although an anatomical database of the deer spine and a detailed comparison with the human spine have been published,[14,15] detailed comparisons of the microarchitecture of spinal cancellous bone between humans and various animal models, including deer, are unavailable. We consider that deer have the following advantages: 1) adult deer are comparable in size to adult humans; 2) they are readily available for research purposes; 3) deer show stable heredity and small interindividual differences; 4) they are hearty, making them good surgical candidates and resistant to infection; and 5) perhaps most importantly, deer have scarcely (if ever) been reported as carriers of prion diseases.

In recent years, quantitative, micro-, and high-resolution computed tomography have proven useful in the assessment of the structural patterns of cancellous bone.[7,8,11,26] However, some researchers[3] consider that traditional bone tissue morphometry is still the optimal method for quantitative analysis of the microarchitecture of cancellous bone. We therefore adopted the 2D bone tissue morphometry method in the current study. Here we measured various morphometric parameters of lumbar cancellous bone from deer and sheep to compare them with those of humans and to explore the feasibility of deer and sheep as models for the human spine.

Materials and Methods

Spine specimens. Spine cadaveric samples were obtained from 3 sources. Spine specimens from 5 adult female deer (age, 1.5 to 2 y; body length, 75 to 95 cm; weight, 75 to 80 kg) euthanized by ketamine overdose were obtained from the Changchun City Shuangyang Area Deer Industry Developing Head Company (Changchun City, China). Spines from 5 adult male merino sheep (age, 1.5 to 2 y; body length, 62 to 79 cm; weight, 46 to 62 kg)

Received: 14 Dec 2009. Revision requested: 25 Jan 2010. Accepted: 27 Mar 2010.
[1]Department of Anatomy, Norman Bethune Medical School, Jilin University, and Departments of [2]spine and [3]hand surgery, the First Affiliated Hospital of Jilin University, Changchun, Jilin Province, China.
[*]Corresponding author. Email: lyqm@email.jlu.edu.cn

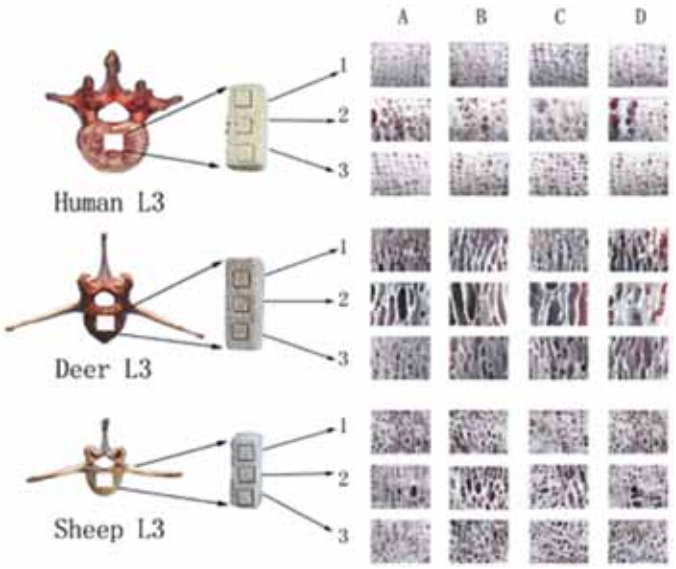

Figure 1. Sampling procedure. One sample was harvested per vertebrae and categorized according to 2 factors for data analysis: species (deer, human, and sheep) and layer (upper [1], middle [2], and lower [3]). Each portion had 4 surfaces: (A) coronal front, (B) coronal rear, (C) sagittal left, and (D) sagittal right. We obtained binary images from the same-size areas of interest (6.10 mm × 5.00 mm) in the center of each surface. Correspondingly, a total of 12 cancellous bone images were obtained for each sample.

euthanized by ketamine overdose were provided by the Experimental Animal Center of Jilin University (Changchun, Jilin Province, China). Spines from 5 men (age, 21 to 31 y; height, 168 to 177 cm) were procured through the Departments of Anatomy of Jilin University. For all spines, intact lumbar specimens (L1 to L6 of deer and sheep, L1 to L5 of humans) were removed en bloc with associated muscles, soft tissues, and intervertebral discs and radiographed to rule out any obvious bone lesions. All procedures involving cadaveric tissue samples conformed to the mandates of and were approved by the local ethics committee and adhered to national standards regarding experimental animals.[17,19,20,21] and the use of human tissues.[18,22]

Acquisition and process of samples. A single cuboidal sample (10 mm × 10 mm × natural height including upper and lower endplates) was obtained from the center of each frozen lumbar vertebral body by using a bone saw (Figure 1). Because vertebrae are predominantly under compressive stress, care was taken to ensure that the long axis of samples was parallel to the vertical axis of the vertebral body. Samples were flushed under low-pressure jet flow with physiologic saline, infiltrated with heparin in physiologic saline (2.5mg/ml), and cleaned by placing in an ultrasonic purifier (TCQ-25, No. 2 Beijing Medical Instrument Factory, Beijing, China) for 20 min. Samples were flushed and sonicated a total of 3 times to ensure complete removal of bone marrow. A total of 85 samples (6 vertebrae per deer and sheep spine; 5 vertebrae per human spine) were selected. Samples were placed in airtight plastic vials stored at –20 °C.[25]

Normal cancellous bone is composed of numerous interlaced bone trabeculae, which range along the physiologic pressure and tension curves.[4] Because the principal loading of vertebrae was compressive loading, investigation of structural morphometric patterns and inhomogeneity trends in the vertical direction was

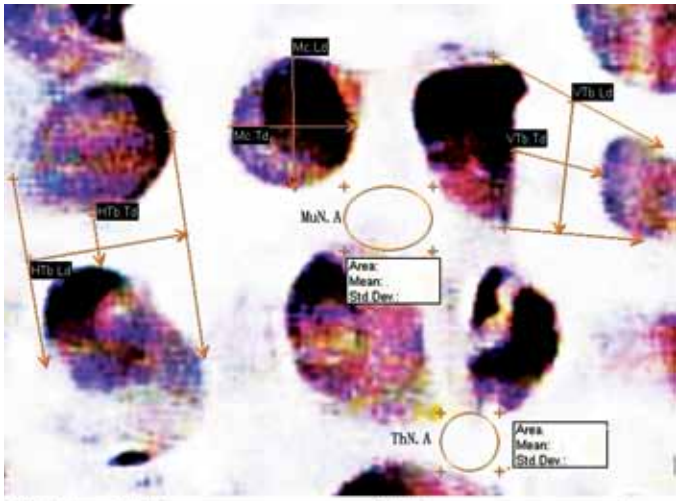

Abbreviation	Parameter	Definition
VTb	Vertical bone trabecula	A trabecula for which the acute angle between the longitudinal diameter of the trabecula and the vertical axis is less than 45°
VTb.N	Vertical bone trabecula number	Total number of vertical trabeculae in the region of interest
VTb.Ld	Vertical bone trabecula longitudinal diameter	Length of the longest line parallel to the vertical axis and running from one side of a vertical trabecula through the medullary canal to the other
VTb.Td	Vertical bone trabecula transverse diameter	Length of the longest line parallel to the horizontal axis and running from one side of a vertical trabecula through the medullary canal to the other
VTb.MI	Vertical bone trabecula morphologic index*	(VTb.Ld – VTb.Td) / VTb.Ld
HTb	Horizontal bone trabecula	A trabecula for which the acute angle between the longitudinal diameter of the trabecula and the horizontal axis is less than 45°
HTb.N	Horizontal bone trabecula number	Total number of horizontal trabeculae in the region of interest
HTb.Ld	Horizontal bone trabecula longitudinal diameter	Length of the longest line parallel to the vertical axis and running from one side of a horizontal trabecula through the medullary canal to the other
HTb.Td	Horizontal bone trabecula transverse diameter	Length of the longest line parallel to the horizontal axis and running from one side of a horizontal trabecula through the medullary canal to the other
HTb.MI	Horizontal bone trabecula morphological index*	(HTb.Ld – HTb.Td) / HTb.Ld
Mc	Medullary canal	Open, nonbone portion of vertebral body
Mc.N	Medullary canal number	Total number of medullary canals in the region of interest
Mc.Ld	Medullary canal longitudinal diameter	Length of the longest line running parallel to the vertical axis from one side of the medullary canal to the other
Mc.Td	Medullary canal transverse diameter	Length of the longest line running parallel to the vertical axis from one side of the medullary canal to the other
Mc.MI	Medullary canal morphological index*	(Mc.Ld – Mc.Td) / Mc.Ld
ThN	3-node	Region of 3 trabeculae joined at their roots
ThN.N	3-node number	Total number of 3-node regions in the region of interest
ThN.A	3-node area	Area of the circular or oval region corresponding to the joined roots of a 3-node region
MuN	Multinode	Region of joined roots of 4 or more trabeculae
MuN.N	Multinode number	Total number of multinode regions in the region of interest
MuN.A	Multinode area	Area of the round or oval region corresponding to the joined roots of a multinode region

*When the value is considerably less than 0 or greater than 1, the trabecula is considered to be platelike in shape; when the value is slightly less or greater than 1, the trabecula is considered to be a columnar structure.

*When the value is less than 0, the medullary canal is considered to be a flat ellipsoid; when the value is greater than 0, the medullary canal is considered to be a long, narrow ellipsoid; when the value is close to 0, the canal is considered to be circular in shape.

Figure 2. Morphometric parameters of lumbar cancellous bone.

important to demonstrate the function of vertebral cancellous bone. Therefore, each vertebral sample was split into an upper, middle, and lower portion from the cranial to caudal side (Figure 1).

Acquisition and processing of binary images. Each vertebral sample was divided into 3 portions (upper, middle, and lower), each of which had 4 surfaces (coronal–front, coronal–hind, sagittal–left, and sagittal–right surface; Figure 1). High-resolution stereo microscopy (CK2, Olympus) was used to select same-size areas of interest (6.10 mm × 5.00 mm; 30.5 mm^2) at the center of each surface and obtain binary images of cancellous bone. The size and position of the region of were determined after comprehensive analysis, to decrease noise and maximize useful histo-

Table 1. Microarchitectural parameters of L3 compared by species

				P		
Parameter	Deer	Human	Sheep	Deer vs human	Sheep vs human	Deer vs sheep
VTb.N	0.752 ± 0.058	0.687 ± 0.030	0.969 ± 0.058	nonsignificant	0.001	0.01
VTb.Ld	1.064 ± 0.018	0.337 ± 0.024	0.745 ± 0.015	0.001	0.001	0.001
VTb.Td	0.343 ± 0.006	0.274 ± 0.008	0.289 ± 0.005	0.001	nonsignificant	0.001
HTb.N	0.305 ± 0.044	0.574 ± 0.023	0.502 ± 0.044	0.001	nonsignificant	0.01
HTb.Ld	0.468 ± 0.012	0.372 ± 0.010	0.517 ± 0.010	0.001	0.001	0.01
HTb.Td	0.411 ± 0.012	0.221 ± 0.011	0.278 ± 0.010	0.001	0.001	0.001
Mc.N	0.592 ± 0.056	0.928 ± 0.025	0.932 ± 0.056	0.001	nonsignificant	0.001
Mc.Ld	1.377 ± 0.025	0.316 ± 0.020	0.848 ± 0.019	0.001	0.001	0.001
Mc.Td	0.569 ± 0.011	0.290 ± 0.009	0.480 ± 0.008	0.001	0.001	0.001
ThN.N	0.326 ± 0.025	0.302 ± 0.013	0.323 ± 0.025	nonsignificant	nonsignificant	nonsignificant
ThN.A	0.079 ± 0.003	0.057 ± 0.003	0.044 ± 0.003	0.001	0.001	0.001
MuN.N	0.107 ± 0.036	0.367 ± 0.018	0.270 ± 0.036	0.001	0.05	0.01
MuN.A	0.272 ± 0.018	0.072 ± 0.009	0.107 ± 0.010	0.001	0.01	0.001

Definitions of parameter abbreviations are found in Figure 2.
Data are presented as the mean (± SE) of all 3 vertebral layers.

logic information and content resolution. In addition, because of known vertical inhomogeneity of the cancellous bone microarchitecture inside vertebra bodies,[1,15] we took care to localize the region of interest at the same location for each surface of each portion of vertebral samples from sheep, deer, and human spine. Thus we obtained 12 images for each sample.

Adobe Photoshop CS (Adobe, San Jose, CA) was used to adjust brightness and edge sharpness to obtain high-definition microarchitectural images of cancellous bone. Cancellous bone was identified by visual inspection of images; to decrease interoperator error, standardized definitions for various morphometric parameters of cancellous bone morphometric formulas were devised (Figure 2). Image analysis software (Efilm Workstation, Merge Healthcare, Hartland, WI) was used to measure these parameters quantitatively.

Statistical methods. Although all images and vertebrae were evaluated, only the data regarding the microarchitecture of L3 in deer, sheep, and humans are shown for the sake of brevity. Data are presented as mean ± SE. All statistical analyses were performed by using SPSS version 17.0 (SPSS Institute, Chicago, IL). Repeated-measures ANOVA was used to compare multiple within-subject factors, which included 'species' (deer, sheep, human) and 'layer' (upper, middle, lower). The least squares difference *t* test was used to compare groups. The significance level was set at a *P* value of less than 0.05.

ANOVA first was performed for the entire lumbar vertebrae, with species as the factor investigated, to search for any differences between the different species across the entire human vertebrae. Then ANOVA was done separately for each layer among the 3 species, again with species as the factor investigated, to determine any differences between species in a single layer. To extend the evaluation, ANOVA was performed separately for each species, with layer as the target factor. The purpose of this analysis was to identify vertical inhomogeneity in a single species.

Results

Comparison of the microarchitecture of L3 in deer, sheep, and humans Although we evaluated L1 through L6 in sheep and deer and L1 through L5 in humans, data regarding the microarchitectural parameters of L3 only are presented (Table 1) for the sake of brevity. Trends and differences apparent through comparison of L3 were mirrored in the remaining vertebrae of each species.

Trends in vertical inhomogeneity of L3. Analyzing and comparing the data for L3 from humans, sheep, and deer by layer (Table 2) provided insight into the vertical inhomogeneity of this vertebra, both within and between species. One noteworthy point that emerged is that differences between layers for deer and sheep tended to be greater than between those in humans (Table 2), indicating greater vertical inhomogeneity in the L3 of the nonhuman species.

Morphologic indices of cancellous bone structure. In human lumbar vertebral cancellous bone, values for the vertical bone trabecula morphologic index of the upper layer were fairly concentrated (79% of values) in the region from 0.2 to 0.7 (that is, corresponding to a columnar morphology; Table 3); only 21% of values were –0.2 to 0.2 or greater 0.7 to 1, indicating that the vertical trabeculae in the upper layer of human L3 were platelike in morphology. The middle and lower layers of human L3 showed similar trends in morphology to the upper layer (Table 3). However, L3 of deer and sheep tended to be platelike in morphology (Table 3), according to the vertical bone trabecula morphologic index. According to the morphologic index, horizontal trabeculae of deer, humans, and sheep L3 tended to be columnar in morphology (Table 3). Whereas the medullary canals of human L3 were distributed approximately equally between flat and long, narrow ellipsoidal morphologies among the upper, middle, and lower vertebral layers, those of deer and sheep tended to be long, narrow ellipsoidal in all 3 layers (Table 3).

Discussion

Microarchitecturally, cancellous bone is a porous network comprising numerous interconnecting columnar or plate-like bone trabeculae. According to Wolff's law,[4] the thickness and length of the trabeculae of normal cancellous bone parallel the physiologic compressive and tension stresses experienced, and the trabeculae of cancellous bone can remodel in orientation, number, and struc-

Table 2. Comparison of microarchitectural parameters (mean ± SE) of each species by layer

	Deer			P			Human			P			Sheep			P		
Parameter	Upper	Middle	Lower	1	2	3	Upper	Middle	Lower	1	2	3	Upper	Middle	Lower	1	2	3
VTb.N	0.856 ± 0.043	0.516 ± 0.057	0.882 ± 0.072	NS	0.001	0.001	0.560 ± 0.062	0.588 ± 0.052	0.690 ± 0.059	NS	NS	NS	1.431 ± 0.062	0.618 ± 0.057	1.196 ± 0.072	0.05	0.001	0.001
VTb.Ld	0.888 ± 0.023	1.334 ± 0.048	1.061 ± 0.024	NS	0.001	0.001	0.383 ± 0.029	0.393 ± 0.061	0.355 ± 0.035	NS	NS	0.05	0.642 ± 0.018	1.125 ± 0.046	0.673 ± 0.021	NS	0.001	0.001
VTb.Td	0.318 ± 0.008	0.424 ± 0.016	0.318 ± 0.018	NS	0.001	0.001	0.222 ± 0.011	0.255 ± 0.020	0.233 ± 0.012	NS	0.01	NS	0.274 ± 0.006	0.370 ± 0.015	0.264 ± 0.007	NS	0.001	0.001
HTb.N	0.382 ± 0.034	0.203 ± 0.052	0.330 ± 0.065	NS	0.001	0.05	0.512 ± 0.053	0.474 ± 0.048	0.618 ± 0.053	NS	NS	NS	0.549 ± 0.059	0.317 ± 0.052	0.621 ± 0.065	NS	0.01	0.001
HTb.Ld	0.496 ± 0.017	0.648 ± 0.029	0.540 ± 0.018	0.001	0.001	0.001	0.377 ± 0.017	0.381 ± 0.048	0.361 ± 0.015	NS	NS	NS	0.471 ± 0.014	0.617 ± 0.023	0.506 ± 0.013	NS	0.001	0.001
HTb.Td	0.346 ± 0.025	0.322 ± 0.020	0.324 ± 0.013	0.001	NS	0.001	0.214 ± 0.025	0.221 ± 0.015	0.226 ± 0.011	NS	NS	NS	0.258 ± 0.021	0.326 ± 0.023	0.272 ± 0.010	NS	0.001	0.01
Mc.N	0.696 ± 0.040	0.408 ± 0.071	0.670 ± 0.076	NS	0.001	0.001	0.887 ± 0.065	0.817 ± 0.049	0.937 ± 0.053	NS	NS	NS	1.284 ± 0.059	0.621 ± 0.071	1.137 ± 0.076	NS	0.001	0.001
Mc.Ld	1.195 ± 0.031	1.772 ± 0.065	1.325 ± 0.036	NS	0.001	0.001	0.323 ± 0.026	0.339 ± 0.046	0.291 ± 0.029	0.05	NS	0.001	0.696 ± 0.023	1.219 ± 0.052	0.816 ± 0.028	0.01	0.001	0.001
Mc.Td	0.563 ± 0.021	0.644 ± 0.021	0.530 ± 0.013	NS	NS	0.01	0.282 ± 0.018	0.327 ± 0.015	0.267 ± 0.011	NS	0.001	0.001	0.441 ± 0.016	0.591 ± 0.017	0.462 ± 0.010	NS	0.001	0.001
ThN.N	0.418 ± 0.052	0.225 ± 0.030	0.333 ± 0.044	NS	0.05	NS	0.334 ± 0.023	0.290 ± 0.023	0.375 ± 0.034	NS	NS	0.01	0.425 ± 0.034	0.193 ± 0.030	0.405 ± 0.044	NS	0.001	0.001
ThN.A	0.056 ± 0.003	0.122 ± 0.008	0.080 ± 0.003	0.01	0.001	0.001	0.052 ± 0.003	0.062 ± 0.008	0.050 ± 0.004	NS	NS	NS	0.039 ± 0.003	0.065 ± 0.008	0.040 ± 0.003	NS	0.001	0.001
MuN.N	0.111 ± 0.020	0.085 ± 0.046	0.134 ± 0.048	NS	NS	0.05	0.375 ± 0.056	0.269 ± 0.036	0.349 ± 0.038	NS	NS	NS	0.428 ± 0.039	0.199 ± 0.046	0.320 ± 0.048	NS	0.001	0.05
MuN.A	0.204 ± 0.016	0.148 ± 0.043	0.242 ± 0.016	NS	0.01	0.01	0.067 ± 0.011	0.076 ± 0.025	0.069 ± 0.011	NS	NS	NS	0.085 ± 0.011	0.156 ± 0.027	0.106 ± 0.011	0.05	0.001	0.05

Definitions of parameter abbreviations are found in Figure 2.
Differences between the P values for a parameter within a species can be interpreted as indicative of vertical inhomogeneity within L3.
KEY: 1, 'Upper vs middle' 2, 'Middle vs lower' 3, 'Upper vs lower'.
[NS] $P > 0.05$ (no significance); [a] $P < 0.05$ (general significance); [b] $P < 0.01$ (middling significance); [c] $P < 0.001$ (remarkable significance)

ture to accommodate and distribute the stresses under which they are placed. The extreme multiplicity, heterogeneity, and anisotropy of the structural shape and spatial arrangement of trabeculae complicate research into the morphometric and mechanical properties of cancellous bone. In the current study, we used traditional bone morphometry techniques and 2-dimensional images to evaluate microarchitectural parameters of the cancellous bone of L3 in humans, sheep, and deer.

Similarities between deer, sheep, and human spinal cancellous bone were greatest among the numbers of vertical and horizontal vertebral trabeculae (Table 1). However, the number of medullary cavities varied markedly among the 3 species (Table 1). Cancellous bone bears about 90% of the load placed on vertebrae.[24] In the human spine, which plays roles in both weight-bearing and load transfer, vertical bone trabeculae follow the lines of compressive stress and are the primary load-bearing structure of vertebral cancellous bone, whereas horizontal bone trabecula are the main structure to conduct the stress and absorb energy. The biomechanical functions of the spine in humans are vastly different from those of deer and sheep. The spines of these species primarily bear load along a single axis, without marked transfer of stress to the periphery. This difference in function accounts for the gradual decrease in the number and size of horizontal trabeculae in this special stress environment.

A fundamental difference among the species is that human trabeculae were characteristically smaller than those of deer and sheep, but for all 3 species the longitudinal diameter of the trabeculae or medullary canals was larger than their transverse diameter, albeit to differing magnitudes (Table 1). In addition, these measures corresponded highly with the data for the morphologic indices of these structures. Our results support the fact that the cancellous bone of the human lumbar spine is an open rod-like network structure of interconnected columnar bone trabeculae, consistent with previous findings.[6,9] In contrast, the cancellous bone of deer and sheep is a parallel plate-like structure connected with plate-like vertebral trabeculae and columnar horizontal trabeculae. Overall, these differences in the characteristics of the horizontal and vertical lumbar cancellous bone microarchitecture reflect the facts that humans are bipedal but deer and sheep are quadrupedal.

To varying degrees, differences in vertical and horizontal inhomogeneity emerged among the 3 species (Table 2), but regardless of species, the middle vertebral layer had more sparsely arranged trabeculae, higher porosity, and lower bone mass than did the upper and lower layers. These characteristics of the cancellous bone of the middle layer reflect its minor role in load bearing.[6] Accordingly, the greatest proportion of load-bearing cortical bone appears along the smallest vertebral cross-section, the middle layer.[5] In contrast, the greatest proportion of cancellous bone appears near the vertebral end plates, which are located in the upper and lower layers. In these layers, cancellous rather than cortical bone bears the greater proportion of the load placed on the vertebrae, and this concentration of stress leads to the denser microarchitectural pattern of the component trabeculae, consistent with a previous report.[5] In addition, several studies[10,27,28] revealed that the microarchitectural pattern of the trabeculae is fine near the end plates but coarse in the center of the vertebra. Use of microcomputed tomography to characterize the trabecular microarchitecture of the cranial, middle, and caudal regions of the ovine L3 vertebra revealed that trabecular number, thickness, spacing,

Table 3. Distribution (% of samples) of calculated microarchitectural morphologic indices by layer and species

Parameter	Calculated vertebral morphology	Upper layer			Middle layer			Lower layer		
		deer	human	sheep	deer	human	sheep	deer	human	sheep
VTb.MI										
	Columnar	41.6%	79.0%	47.5%	34.2%	78.1%	46.0%	37.8%	78.3%	50.5%
	Plate-like	58.4%	21.0%	52.5%	65.8%	21.9%	54.0%	62.2%	21.7%	49.5%
HTb.MI										
	Columnar	72.0%	73.6%	68.5%	77.4%	79.4%	66.0%	60.0%	69.7%	62.8%
	Plate-like	28.0%	26.4%	31.5%	22.6%	20.6%	34.0%	40.0%	30.3%	37.2%
Mc.MI										
	Flat ellipsoid	9.0%	58.1%	22.1%	4.0%	49.0%	16.3%	6.3%	44.2%	15.5%
	Long, narrow ellipsoid	91.0%	41.9%	77.9%	96.0%	51.0%	83.7%	93.7%	55.8%	84.5%

Definitions of parameter abbreviations are found in Figure 2.

connectivity density, degree of anisotropy, and bone mineral density all varied significantly between regions.[16] Our results basically confirm these findings, and the observed differences were consistent with the biomechanical hypothesis that in vivo loads are distributed differently at the endplates compared with the midvertebra.

The 2D image quantitative analysis method we used to evaluate the microstructural patterns of the cancellous bone of the deer, sheep, and human lumbar spine offered the following advantages, compared with qualitative, high-resolution, or micro-computed tomography analysis. With our method, (1) it was easy to distinguish the vertical and horizontal bone trabeculae of cancellous bone and measure their number and relative structural parameters; (2) the number and structural parameters of medullary canals could be analyzed; and (3) the relation between various structural categories, numbers of various structures, and area of nodes in cancellous bone could be analyzed. However, our method has several drawbacks. We had to obtain binary images of bone tissue directly from the 4 surfaces of samples instead of from resin-embedded, sectioned samples. Although we might acquire higher-resolution images from the nonembedded samples, they are not amenable to subsequent mechanical testing and density measurement. Therefore we could not obtain bone tissue images from samples that may have become damaged. In addition, we were unable to evaluate 3D spatial patterns of cancellous bone through binary images. To compensate for this deficiency, we devised new structural parameters (such as the morphologic index) to estimate the spatial morphologic patterns of cancellous bone.

Our current study provides a thorough microarchitectural database of the lumbar spinal vertebrae of deer and sheep and their detailed comparison with the human lumbar spine. Our results show that, according to the bone morphometric methods we used, both deer and sheep both offer viable options as models of the human spine. The biomechanics of cancellous bone in deer and sheep vertebrae should be studied further, to increase the accurate interpretation of results of studies using these animal models of the human spine.

Acknowledgments

We than the Changchun City Shuangyang Area Deer Industry Developing Head Company and the Experimental Animal Center of Jilin University for providing the deer and sheep spine specimens. We acknowledge the Departments of Anatomy of Jilin University for providing the fresh cadavers and the place where work was conducted. We also acknowledge the Department of Spine Surgery of the First Affiliated Hospital of Jilin University for allowing us to use the image analysis software. The authors thank Mr Debao Zhen, Mr Qing Tian, and Miss Chunfang Gao for their suggestions concerning the use of English in this manuscript.

References

1. **Banse X, Devogelaer JP, Munting E, Delloye C, Cornu O, Grynpas M.** 2001. Inhomogeneity of human vertebral cancellous bone: systematic desity and structure patterns inside the vertebral body. Bone **28:**563–571.
2. **Christensen FB, Dalstra M, Sejling F, Overgaard S, Bünger C.** 2000. Titanium alloy enhances bone–pedicle screw fixation: mechanical histomorphometrical results of titanium alloy versus stainless steel. Eur Spine J **9:**97–103.
3. **Cortet B, Colin D, Dubois P, Delcambre B, Marchandise X.** 1995. Methods for quantitative analysis of trabecular bone structure. Rev Rhum Engl Ed **62:**781–793.
4. **Cowin SC.** 1986. Wolff's law of trabecular architecture at remodeling equilibrium. J Biomech Eng **108:**83–88.
5. **Eswaran SK, Gupta A, Adams MF, Keaveny TM.** 2006. Cortical and trabecular load sharing in the human vertebral body. J Bone Miner Res **21:**307–314.
6. **Gibson LJ.** 1985. The mechanical behaviour of cancellous bone. J Biomech **18:**317–328.
7. **Gordon CL, Lang TF, Augat P, Genant HK.** 1998. Image-based assessment of spinal trabecular bone structure from high-resolution CT images. Osteoporos Int **8:**317–325.
8. **Gordon CL, Webber CE, Adachi JD, Christoforou N.** 1996. In vivo assessment of trabecular bone structure at the distal radius from high-resolution computed tomography image. Phys Med Biol **41:**495–508.
9. **Hildebrand T, Laib A, Müller R, Dequeker J, Rüegseger P.** 1999. Direct 3-dimensional morphometric analysis of human cancellous bone: microstructural data from spine, femur, iliac crest, and calcaneus. J Bone Miner Res **14:**1167–1174.
10. **Jayasinghe JA, Jones SJ, Boyde A.** 1994. Three-dimensional photographic study of cancellous bone in human fourth lumbar vertebral bodies. Anat Embryol (Berl) **189:**259–274.
11. **Jiang Y, Zhao J, Augat P, Ouyang X, Lu Y, Majumdar S, Genant HK.** 1998. Trabecular born mineral and calculated structure of human bone specimens scanned by peripheral quantitative computed tomography: relation to biomechanical properties. J Bone Miner Res **13:**1783–1790.
12. **Kennedy OD, Brennan O, Rackard SM, O'Brien FJ, Taylor D, Lee TC.** 2009. Variation of trabecular microzrchitectural parameters in

cranial, caudal, and midvertebral regions of the ovine L3 vertebra. J Anat **214:**729–735.
13. **Kettler A, Liakos L, Haegele B, Wilke HJ.** 2007. Are the spines of calf, pig, and sheep suitable models for preclinical implant tests? Eur Spine J **16:**2186–2192.
14. **Kumar N, Kukreti S, Ishaque M, Mulholland R.** 2000. Anatomy of deer spine and its comparison to the human spine. Anat Rec **260:**189–203.
15. **Kumar N, Kukreti S, Kukreti S, Ishaque M, Sengupta DK, Mulholland RC.** 2002. Functional anatomy of the deer spine:an appropriate biomechanical model for the human spine? Anat Rec **266:**108–117.
16. **Ministry of Agriculture, Fisheries, and Food**. 1998. Bovine spongiform encephalopathy in Great Britain. A progress report. London (UK): MAFF.
17. **People's Republic of China Ministry of Health**. 1989. Administrative rules of experimental animals. Beijing (China): Ministry of Health.
18. **People's Republic of China Ministry of Health.** 1994. Regulations for medical institutions. Beijing (China): Ministry of Health.
19. **People's Republic of China National Science and Technology Committee**. 1988. The regulations of experimental animals. Beijing (China): State Science and Technology Commission.
20. **People's Republic of China National Science and Technology Committee**. 1997. Experimental animals national standards. Beijing (China): State Science and Technology Commission.
21. **People's Republic of China National Standards.** 1995. Publishing house of China standards: experimental animals national standards. Beijing (China): State Science and Technology Commission.
22. **People's Republic of China State Department.** 2004. Regulations for biosafety of pathogenic laboratories. Beijing (China): State Council.
23. **Sandén B, Olerud C, Larsson C.** 2001. Hydroxyapatite coating enhances fixation of loaded pedicle screws: a mechanical in vivo study in sheep. Eur Spine J **10:**334–339.
24. **Schaffner G, Guo XD, Silva MJ, Gibson LJ.** 2000. Modeling fatigue damage accumulation in 2-dimensional Voronoi honeycombs. International Journal of Mechanical Sciences **42:**645–656.
25. **Sedlin ED, Hirsch C.** 1966. Factors affecting the determination of the physical properties of the femoral cortical bone. Acta Orthop Scand **37:**29–48.
26. **Strohm PC, Kubosch D, Bley TA, Sprecher CM, Südkamp NP, Milz S.** 2008. Detection of bone graft failure in lumbar spondylodesis: spatial esolution with high-resolution peripheral quantitative CT. Am J Roentgenol **190:**1255–1259.
27. **Tan J, Wan WP, Zhou XH, Xu JW, Jia LS.** 2001. Quantitative imaging analysis of lumbar vertebral trbecular architecture with high resolution CT. Orthop J Chin **8(8):**780–782.
28. **Wang MP, Tan J, Wu WL, Zhang GZ, Zhu HM.** 1996. Quantitative image analysis of vertebral body architecture. Chin J Osteoporos **2(3):**1–4.
29. **Wells GA, Hawkins SA, Green RB, Austin AR, Dexter I, Spencer YI, Chaplin MJ, Stack MJ, Dawson M**. 1998. Preliminary observations on the pathogenesis of experimental bovine spongiform encephalopathy (BSE): an update. Vet Rec **142:**103–106.
30. **Wilke HJ, Kettler A, Wenger KH.** 1997. Anatomy of the sheep spine and its comparison to the human spine. Anat Rec **247:**542–555.
31. **Yildirim OS, Aksakal B, Hanyaloglu SC, Erdogan F, Okur A.** 2006. Hydroxyapatite dip coated and uncoated titanium polyaxial pedicle screws: an in vivo bovine model. Spine **31:**E215–E220.
32. **Zhao ZD.** 2008. Biomechanical analysis of spinal implants. J Clin Rehab Tissue Eng Res **12(35):**6915–6918.